Advances in Sustainable Petroleum Engineering Science ISSN 1937-7991
Volume 2, Number 3

DEVELOPMENT OF NEW SCALING CRITERIA FOR A FLUID FLOW MODEL WITH MEMORY

M. Enamul Hossain*[1] and M. Rafiqul Islam[2]

[1]Department of Petroleum Engineering
King Fahd University of Petroleum & Minerals (KFUPM)
Dhahran 31261, Saudi Arabia
[2]Department of Civil Engineering, Dalhousie University
Barrington Street, Halifax, NS, Canada, B3J-1Z1

ABSTRACT

New scaling criteria for an oil-water displacement process are presented in this paper. The modified Darcy law with incorporating fluid memory is used to develop the model equation. The mathematical model development of different scaling criteria for a variety of scaling options is outlined here. Sets of similarity groups are derived by inspectional and dimensional analysis for the displacement process using fluid memory concept. To date there has been no rigorous presentation of the scaling requirements for a displacement process where fluid memory has been counted. Relaxed sets of scaling criteria based on major mechanisms of a process are determined. The purpose of this paper is to present a method of developing a set of scaling criteria which permits different relationships between saturation, capillary pressure, fluid pressure, and velocities involving fluid memory in the model and prototype. The most efficient approach is identified for oil-water displacement process when fluid memory has been taken care. This new citation of idea can be used in enhanced oil recovery scheme where formation and fluid properties are more complex in explaining their behavior.

Keywords: inspectional and dimensional analysis, displacement process, porous media, prototype, model.

NOMENCLATURE

A_{yz} = cross sectional area of reservoir, ft^2
f_o = ratio of oil phase velocity to total velocity, u_{ox} / U_x
f_w = ratio of water phase velocity to total velocity, u_{wx} / U_x

* Corresponding author: Email: menamul@kfupm.edu.sa; dr.mehossain@gmail.com

g= gravitational acceleration, $ft/\ s^2$
H = height of the formation, ft
$J(S)$= dimensionless function
k_o= reservoir permeability when fluid is oil, *md*
k_w= reservoir permeability when fluid is water, *md*
L= Length of the formation, ft
p= current reservoir pressure (at time *t*), *psia*
p_c= capillary pressure of the reservoir, *psia*
p_o= oil pressure, *psia*
p_w= water pressure, *psia*
p_i= initial reservoir pressure, *psia*
S_o= oil saturation at p, dimensionless
S_w= water saturation at p, dimensionless
S_{oi}= oil saturation at initial pressure p_i, dimensionless
S_{wi}= water saturation at initial pressure p_i, dimensionless
t= time, *hr*
u_o= reservoir oil velocity, ft/s
u_w= reservoir water velocity, ft/s
u_x= fluid velocity in porous media in the direction of x axis, ft/s
U_x= algebraic summation of reservoir oil and water velocity in *x*-direction, ft/s
u_{wx}= reservoir water velocity in *x*-direction, ft/s
W= width of the formation, *ft*
x= variable position from the wellbore along x-direction, ft
z= vertical distance from reservoir ground surface toward centre of the earth along z-direction, ft
α = fractional order of differentiation, dimensionless
ξ = a dummy variable for time i.e. real part in the plane of the integral, *s*
η= ratio of the pseudopermeability of the medium with memory to fluid viscosity, $ft^3\ s^{1+\alpha}/lb_m$
η_o= ratio of the pseudopermeability of the medium with memory to oil viscosity, $ft^3\ s^{1+\alpha}/lb_m$
η_w= ratio of the pseudopermeability of the medium with memory to water viscosity, $ft^3\ s^{1+\alpha}/lb_m$
ρ_o = density of oil at pressure $p,\ lb_m/ft^3$
ρ_w = density of water at pressure $p,\ lb_m/ft^3$
ϕ = porosity of the solid rock media, dimensionless
θ = contact angle
σ = interfacial tension, lb_m/s^2
μ = fluid dynamic viscosity, $lb_f s/ft^2$
Γ= gamma function

Subscript

D = dimensionless quantity
R = reference quantity
o = oil
w = water
xo = oil in x-direction
yo = oil in y-direction
zo = oil in z-direction

xw = water in x-direction
yw = water in y-direction
zw = water in z-direction

INTRODUCTION

Laboratory experiments are the most useful way of developing predictive models for various engineering applications. The usage of scaled laboratory models to simulate field conditions such as petroleum reservoirs are known to be efficient in evaluating the advantages of a recovery process (Coskuner and Bentsen, 1988). This procedure would be well accepted when scaling laws would be known in order to scale up laboratory results to field conditions. This scaling up offers a formidable challenge in scenarios involving complex solid-fluid, fluid-fluid interactions, which are predominant in a displacement process, such as in enhanced oil recovery (EOR) of petroleum engineering. In scaling such miscible displacements, an inspectional analysis, complemented by dimensional analysis is utilized to obtain a set of scaling criteria (Pozzi and Blackwell, 1963). A scaled model is designed on the basis of the principle of similarity. Such a model is characterized by the same ratios of dimensions, forces, velocities, and temperature. The model geometry, pressure drop, flow rate, time factor, etc are different for different approaches depending on the type of scaling criteria used. Each approach has its unique advantages and disadvantages (Bansal and Islam, 1994). Therefore, the performance of any displacement process in porous media is governed by the related variables. These variables can be combined by dimensionless groups.

It should be noted that the complete set of scaling criteria is very difficult to satisfy. Therefore, some of the similarity groups must be relaxed in order to satisfy the most important parameter of the specific reservoir activities. The choice of which requirements to relax depends on the particular process being modeled. Scaling of the phenomena considered to be least important to a particular process might be relaxed without significantly affecting the major features of the process. The choice of an approach depends on the importance of the phenomena that are not scaled by that approach. As an example, if one considers such an approach where, model and prototype have the same morphology, the same fluids, and are operated at the same conditions of pressure and temperature, the scaling groups such as geometric factors, morphology factors, ratio of gravitational to viscous forces are completely satisfied. The criteria used most widely for high pressure models are outlined by Pujol and Boberg (1972). The high pressure models typically employ the same fluids in the model as found in the prototype field (Kimber et al., 1988).

There are two basic available methods in the literature by which the dimensionless groups can be obtained (Geertsma et al., 1956; Loomis and Crowell, 1964; Rojas, 1985; Islam, 1987). The methods used are inspectional analysis and dimensional analysis. They have discussed extensively the methods and their applications in the petroleum industry. The researchers mainly focused their works on oil displacements and recovery processes (Pujol and Boberg, 1972; Farouq Ali and Redford, 1977; Lozada and Farouq Ali, 1987; Lozada and Farouq Ali, 1988; Kimber et al., 1988; Islam and Farouq Ali, 1990; Islam and Farouq Ali, 1992; Bansal and Islam, 1994; Islam et al., 1994; Sundaram and Islam, 1994). Basu and Islam (2007) studied a scaling up of chemical injection experiments. They presented a series of chemical adsorption tests and provide one with the scaled up versions. They gave a guideline how to interpret laboratory experimental results and apply the scaling laws to predict field behavior. They also compared their findings with numerical simulation results. However, Scaled physical models have been reported to be more desirable than numerical simulations (Farouq Ali et al., 1987). This is largely applicable for recovery methods where phase equilibrium and gravitational forces are significant factors.

Recently, Hossain et al. (2009a) studied the scaling criteria for designing waterjet drilling laboratory experiments for reasonably simulating a given oilfield operation. They proposed a scaling approach and derived the dimensionless groups for the waterjet drilling technique. A scaled model is developed including a complete set of similarity groups where experimental results are scaled up for field application. In addition, empirical models for the depth (*D*) and rate of penetration (*ROP*) are established based on scaled-up process for a drilling oil field application. However, there is no available literature or model that deals with the scaling criteria and its applications based on displacement process with memory concept. The objectives of this paper are to study the relevant variables engaged in displacement process where the notion of memory is considered during the development of the model equation. Finally dimensionless groups, relaxed sets of similarity groups and an efficient approach are identified using inspectional and dimensional analysis. In future, the usage of prototypes are proposed for proper selection of a subset of scaling groups that may adequately represent the significant physical interactions dominant in the displacement process. The choice of the subset should be applicable to dimensionless groups which may annul the effect of the parameters and do not contribute adequately to the fluid-fluid displacement process.

MODEL DESCRIPTION

A reservoir surrounded with known geometry contains only oil and water. The flow is parallel to all-axis (Figure 1). The pressure and saturation are uniform throughout the reservoir. The pore space is assumed to be completely filled with oil and water.

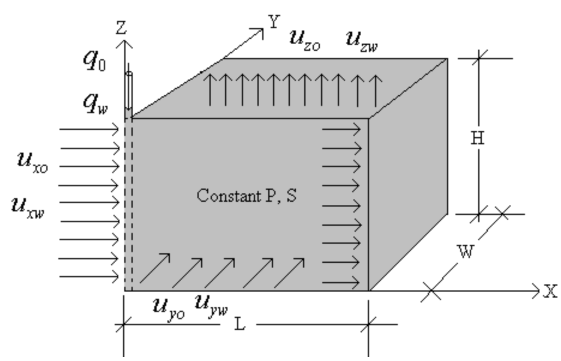

Figure 1. Porous media considering its state.

Water is injected at one end maintaining a given constant filtration velocities u_{1o}, u_{1w}. Just before the production starts up, the saturation and pressure of oil and water is known. The injection well is in the center of the reservoir and production well surrounds the injection well. The injection and production of water and oil is at a definite rate or pressure. The oil and water components are assumed to be immiscible, therefore, there is no mass transfer between the oil and water phase. In addition, there is no slippage in flow. Moreover, it is assumed that there is no effect of capillary pressure and initially both fluids are incompressible and have constant viscosities.

DERIVATION OF MATHEMATICAL MODEL

Let us consider the modified Darcy law with fluid memory for both oil and water phase during the production. The equations of state for each fluid, relationship between the capillary pressure and saturation have been presented as constitutive relationships and constrains in Table 1. A model can be developed for displacement of oil by water in the porous media by using the modified Darcy law (Hossain et al., 2007; Hossain et al., 2008; Hossain et al., 2009b) with fluid memory which may be written as

$$u_x = -\eta \left[\frac{\partial^\alpha}{\partial t^\alpha}\left(\frac{\partial p}{\partial x}\right)\right] \tag{1}$$

where, $\frac{\partial^\alpha}{\partial t^\alpha}\left(\frac{\partial p}{\partial x}\right) = \frac{\int_0^t (t-\xi)^{-\alpha}\left(\frac{\partial^2 p}{\partial \xi\, \partial x}\right) d\xi}{\Gamma(1-\alpha)}$, with $0 \leq \alpha < 1$.

Table 1. Constitutive relationship and constraints

Constitutive relationship and constraints	
1.	$\rho_o = \rho_o(p_o)$
2.	$\rho_w = \rho_w(p_w)$
3.	$\eta_o = \eta_o(k_o, \mu_o, p_o)$
4.	$\eta_w = \eta_w(k_w, \mu_w, p_w)$
5.	$\phi \cong$ constant
6.	$S_o + S_w = 1$
7.	$p_o - p_w = p_c(S_o, S_w, \theta_o, \theta_w, \sigma, k)$

Equation (1) can be written as

$$u_x = -\eta \frac{\int_0^t (t-\xi)^{-\alpha}\left(\frac{\partial^2 p}{\partial \xi\, \partial x}\right) d\xi}{\Gamma(1-\alpha)} \tag{2}$$

Equation (2) can be written for oil and water as

$$u_{xo} = -\frac{\eta_o}{\Gamma(1-\alpha)} \int_0^t (t-\xi)^{-\alpha}\left(\frac{\partial^2 p_o}{\partial \xi\, \partial x}\right) d\xi \tag{3}$$

$$u_{xw} = -\frac{\eta_w}{\Gamma(1-\alpha)} \int_0^t (t-\xi)^{-\alpha}\left(\frac{\partial^2 p_w}{\partial \xi\, \partial x}\right) d\xi \tag{4}$$

The continuity equation in terms of the phase saturation equation, which is a control on the sum of phase saturations, can be written as

$$div(\rho_o\, u_o) + \phi \frac{\partial(\rho_o\, S_o)}{\partial t} = 0 \tag{5}$$

$$div(\rho_w\, u_w) + \phi \frac{\partial(\rho_w\, S_w)}{\partial t} = 0 \tag{6}$$

where, in Cartesian coordinates, $div(u) = \frac{\partial u_x}{\partial x} + \frac{\partial u_y}{\partial y} + \frac{\partial u_z}{\partial z}$. In the beginning of the reservoir, a simple material balance for incompressible fluids, and for each phase, Eqs. (5) and (6) in *x*-direction only can be written as

$$\frac{\partial u_{xo}}{\partial x} + \phi \frac{\partial S_o}{\partial t} = 0 \tag{7}$$

$$\frac{\partial u_{xw}}{\partial x} + \phi \frac{\partial S_w}{\partial t} = 0 \tag{8}$$

Here, u_{xo} and u_{xw} are the algebraic values of the components of the filtration velocities in *x*-direction. These are considered because the components on other axis are assumed as zero. The above equations can be transformed by taking as a new variables U_x, f_o, and f_w where $u \neq 0$. These variables can be defined as

$$U_x = u_{xo} + u_{xw} \tag{9}$$

$$f_o = \frac{u_{xo}}{U_x} \tag{10}$$

$$f_w = 1 - f_o = \frac{u_{xw}}{U_x} \tag{11}$$

Substituting Eqs. (10) and (11) into Eqs. (3) and (4) respectively.

$$U_x\, f_o = -\frac{\eta_o}{\Gamma(1-\alpha)} \int_0^t (t - \xi)^{-\alpha} \left(\frac{\partial^2 p_o}{\partial \xi\, \partial x}\right) d\xi \tag{12}$$

$$U_x(1 - f_o) = -\frac{\eta_w}{\Gamma(1-\alpha)} \int_0^t (t - \xi)^{-\alpha} \left(\frac{\partial^2 p_w}{\partial \xi\, \partial x}\right) d\xi \tag{13}$$

The capillary pressure relation (Eq. (7) of Table 1) can be differentiated with respect to

$$x\, \frac{\partial p_o}{\partial x} - \frac{\partial p_w}{\partial x} = \frac{\partial p_c}{\partial x}$$

Again differentiating the above equation with respect to ξ

$$-\frac{\partial^2 p_w}{\partial \xi \partial x} = \frac{\partial^2 p_c}{\partial \xi \partial x}$$

$$\frac{\partial^2 p_o}{\partial \xi \partial x} = \frac{\partial^2 p_w}{\partial \xi \partial x} + \frac{\partial^2 p_c}{\partial \xi \partial x} \tag{14}$$

Substituting Eq. (14) in Eq. (12) and adding the Eqs. (12) and (13)

$$U_x = -\frac{\eta_o}{\Gamma(1-\alpha)}\int_0^t (t-\xi)^{-\alpha}\left[\frac{\partial^2 p_w}{\partial\xi\partial x}+\frac{\partial^2 p_c}{\partial\xi\partial x}\right]d\xi - \frac{\eta_w}{\Gamma(1-\alpha)}\int_0^t (t-\xi)^{-\alpha}\left[\frac{\partial^2 p_w}{\partial\xi\partial x}\right]d\xi$$

$$U_x = -\frac{\eta_o}{\Gamma(1-\alpha)}\int_0^t (t-\xi)^{-\alpha}\left[\frac{\partial^2 p_c}{\partial\xi\partial x}\right]d\xi - \frac{\eta_o+\eta_w}{\Gamma(1-\alpha)}\int_0^t (t-\xi)^{-\alpha}\left[\frac{\partial^2 p_w}{\partial\xi\partial x}\right]d\xi \tag{15}$$

Substituting Eq. (11) in Eq. (8)

$$\frac{\partial}{\partial x}(1-f_o)U_x + \phi\frac{\partial S_w}{\partial t} = 0$$
$$(1-f_o)\frac{\partial U_x}{\partial x} + U_x(1-f_o)\frac{\partial(1-f_o)}{\partial x} + \phi\frac{\partial S_w}{\partial t} = 0$$

Since, $\frac{\partial U_x}{\partial x} = 0$, the above equation becomes

$$-U_x(1-f_o)\frac{\partial f_o}{\partial x} + \phi\frac{\partial S_w}{\partial t} = 0 \tag{16}$$

Substituting Eq. (15) in Eq. (16)

$$-\left\{-\frac{\eta_o}{\Gamma(1-\alpha)}\int_0^t (t-\xi)^{-\alpha}\left[\frac{\partial^2 p_c}{\partial\xi\partial x}\right]d\xi - \frac{\eta_o+\eta_w}{\Gamma(1-\alpha)}\int_0^t (t-\xi)^{-\alpha}\left[\frac{\partial^2 p_w}{\partial\xi\partial x}\right]d\xi\right\}(1-f_o)\frac{\partial f_o}{\partial x} + \phi\frac{\partial S_w}{\partial t} = 0$$

$$\left\{\frac{\eta_o}{\Gamma(1-\alpha)}\int_0^t (t-\xi)^{-\alpha}\left[\frac{\partial}{\partial\xi}\left(\frac{\partial p_c}{\partial S_w}\frac{\partial S_w}{\partial x}\right)\right]d\xi + \frac{\eta_o+\eta_w}{\Gamma(1-\alpha)}\int_0^t (t-\xi)^{-\alpha}\left[\frac{\partial^2 p_w}{\partial\xi\partial x}\right]d\xi\right\}(1-f_o)\frac{\partial f_o}{\partial x} + \phi\frac{\partial S_w}{\partial t} = 0 \tag{17}$$

In three dimensional form, Eq. (17) can be written as

$$\left\{\frac{\eta_o}{\Gamma(1-\alpha)}\int_0^t (t-\xi)^{-\alpha}\left[\frac{\partial}{\partial\xi}\left(\frac{\partial p_c}{\partial S_w}\frac{\partial S_w}{\partial x}\right)\right]d\xi + \frac{\eta_o+\eta_w}{\Gamma(1-\alpha)}\int_0^t (t-\xi)^{-\alpha}\left[\frac{\partial^2 p_w}{\partial\xi\partial x}\right]d\xi\right\}(1-f_{ox})\frac{\partial f_{ox}}{\partial x}$$

$$+\left\{\frac{\eta_o}{\Gamma(1-\alpha)}\int_0^t (t-\xi)^{-\alpha}\left[\frac{\partial}{\partial\xi}\left(\frac{\partial p_c}{\partial S_w}\frac{\partial S_w}{\partial y}\right)\right]d\xi + \frac{\eta_o+\eta_w}{\Gamma(1-\alpha)}\int_0^t (t-\xi)^{-\alpha}\left[\frac{\partial^2 p_w}{\partial\xi\partial y}\right]d\xi\right\}(1-f_{oy})\frac{\partial f_{oy}}{\partial y}$$

$$+\left\{\frac{\eta_o}{\Gamma(1-\alpha)}\int_0^t (t-\xi)^{-\alpha}\left[\frac{\partial}{\partial\xi}\left(\frac{\partial p_c}{\partial S_w}\frac{\partial S_w}{\partial z}\right)\right]d\xi + \frac{\eta_o+\eta_w}{\Gamma(1-\alpha)}\int_0^t (t-\xi)^{-\alpha}\left[\frac{\partial^2 p_w}{\partial\xi\partial z}\right]d\xi\right\}(1-f_{oz})\frac{\partial f_{oz}}{\partial z}$$

$$+\rho_o g\, z + \phi\frac{\partial S_w}{\partial t} = 0 \tag{18}$$

Equation (18) presents a simple oil-water displacement model with memory in a 3D system at any time, t for a production reservoir.

DEVELOPMENT OF DIMENSIONLESS FORM

The dimensionless forms of model equation, corresponding or related equations and initial and boundary conditions are necessary for inspectional analysis. In developing the dimensionless similarity groups using inspectional analysis, each variable or properties in Eqs. (9-11) and (18) and in Table 1 can be written in dimensionless form by dividing it with some characteristic reference quantity. For example, the property M, $M_D = M/M_R$, where M_D is the dimensionless form of property M, and M_R is some constant characteristic reference quantity. Therefore the equations become;

Eq. (9):

$$U_R U_{xD} = u_{xoR}\ u_{xoD} + u_{xwR}\ u_{xwD}$$

$$U_{xD} = \left(\frac{u_{xoR}}{U_R}\right) u_{xoD} + \left(\frac{u_{xwR}}{U_R}\right) u_{xwD} \tag{19}$$

Similarly in *y* and *z*-direction

$$U_{yD} = \left(\frac{u_{yoR}}{U_R}\right) u_{yoD} + \left(\frac{u_{ywR}}{U_R}\right) u_{ywD} \text{ and } U_{zD} = \left(\frac{u_{zoR}}{U_R}\right) u_{zoD} + \left(\frac{u_{zwR}}{U_R}\right) u_{zwD} \tag{20}$$

Eq. (10):

$$f_{oR}\ f_{oxD} = \frac{u_{oxR}\ u_{oxD}}{U_R\ U_{xD}}$$

$$f_{oxD} = \left(\frac{u_{oxR}}{U_R\ f_{oR}}\right)\frac{u_{oxD}}{U_{xD}} \tag{21}$$

Similarly in *y* and *z*-direction

$$f_{oyD} = \left(\frac{u_{oyR}}{U_R\ f_{oR}}\right)\frac{u_{oyD}}{U_{xD}} \text{ and } f_{ozD} = \left(\frac{u_{ozR}}{U_R\ f_{oR}}\right)\frac{u_{ozD}}{U_{xD}} \tag{22}$$

Eq. (11):

$$f_{wR}\ f_{wxD} = \frac{u_{wxR}\ u_{wxD}}{U_R\ U_{xD}}$$

$$f_{wxD} = \left(\frac{u_{wxR}}{U_R\ f_{wR}}\right)\frac{u_{wxD}}{U_{xD}} \tag{23}$$

Similarly in *y* and *z*-direction

$$f_{wyD} = \left(\frac{u_{wyR}}{U_R\ f_{wR}}\right)\frac{u_{wyD}}{U_{xD}} \text{ and } f_{wzD} = \left(\frac{u_{wzR}}{U_R\ f_{wR}}\right)\frac{u_{wzD}}{U_{xD}} \tag{24}$$

Eq. (18):

$$\left\{\begin{array}{l} \frac{\eta_R\ \eta_{oD}}{\Gamma(1-\alpha)} \int_0^{t_R t_D} (t_R t_D - \xi_R \xi_D)^{-\alpha} \left[\frac{p_{cR}}{x_R} \frac{\partial}{\partial \xi_D}\left(\frac{\partial p_{cD}}{\partial S_{wD}} \frac{\partial S_{wD}}{\partial x_D}\right)\right] d\xi_D \\ + \frac{\eta_R\ \eta_{oD} + \eta_R\ \eta_{wD}}{\Gamma(1-\alpha)} \int_0^{t_R t_D} (t_R t_D - \xi_R \xi_D)^{-\alpha} \left[\frac{p_{wR}}{x_R}\ \frac{\partial^2 p_{wD}}{\partial \xi_D \partial x_D}\right] d\xi_D \end{array}\right\} (1 - f_{oR} f_{oxD}) \frac{f_{oR}}{x_R} \frac{\partial f_{oxD}}{\partial x_D}$$

$$+\left\{\begin{array}{l}\frac{\eta_R\,\eta_{oD}}{\Gamma(1-\alpha)}\int_0^{t_R t_D}(t_R t_D-\ \xi_R\xi_D)^{-\alpha}\left[\frac{p_{cR}}{y_R}\frac{\partial}{\partial\xi_D}\left(\frac{\partial p_{cD}}{\partial S_{wD}}\frac{\partial S_{wD}}{\partial y_D}\right)\right]d\xi_D\\+\frac{\eta_R\,\eta_{oD}+\eta_R\,\eta_{wD}}{\Gamma(1-\alpha)}\int_0^{t_R t_D}(t_R t_D-\ \xi_R\xi_D)^{-\alpha}\left[\frac{p_{wR}}{y_R}\frac{\partial^2 p_{wD}}{\partial\xi_D\partial y_D}\right]d\xi_D\end{array}\right\}(1-f_{oR}f_{oyD})\frac{f_{oR}}{y_R}\frac{\partial f_{oyD}}{\partial y_D}$$

$$+\left\{\begin{array}{l}\frac{\eta_R\,\eta_{oD}}{\Gamma(1-\alpha)}\int_0^{t_R t_D}(t_R t_D-\ \xi_R\xi_D)^{-\alpha}\left[\frac{p_{cR}}{z_R}\frac{\partial}{\partial\xi_D}\left(\frac{\partial p_{cD}}{\partial S_{wD}}\frac{\partial S_{wD}}{\partial z_D}\right)\right]d\xi_D\\+\frac{\eta_R\,\eta_{oD}+\eta_R\,\eta_{wD}}{\Gamma(1-\alpha)}\int_0^{t_R t_D}(t_R t_D-\ \xi_R\xi_D)^{-\alpha}\left[\frac{p_{wR}}{z_R}\frac{\partial^2 p_{wD}}{\partial\xi_D\partial z_D}\right]d\xi_D\end{array}\right\}(1-f_{oR}f_{ozD})\frac{f_{oR}}{z_R}\frac{\partial f_{ozD}}{\partial z_D}$$

$$+\rho_{oR}\rho_{oD}\,g_R g_D z_R z_D+\frac{\phi_R S_{wR}}{t_R}\phi_D\frac{\partial S_{wD}}{\partial t_D}=0$$

$$\left\{\frac{\eta_R\,\eta_{oD}}{\Gamma(1-\alpha)t_R^\alpha}\frac{f_{oR}\ p_{cR}}{x_R^2}\int_0^{t_R t_D}(t_D-\ \xi_D)^{-\alpha}\left[\frac{\partial}{\partial\xi_D}\left(\frac{\partial p_{cD}}{\partial S_{wD}}\frac{\partial S_{wD}}{\partial x_D}\right)\right]d\xi_D\right\}(1-f_{oR}f_{oxD})\frac{\partial f_{oxD}}{\partial x_D}$$

$$+\left\{\frac{\eta_R\,\eta_{oD}+\eta_R\,\eta_{wD}}{\Gamma(1-\alpha)\,t_R^\alpha}\frac{f_{oR}\ p_{wR}}{x_R^2}\int_0^{t_R t_D}(t_D-\ \xi_D)^{-\alpha}\left[\frac{\partial^2 p_{wD}}{\partial\xi_D\partial x_D}\right]d\xi_D\right\}(1-f_{oR}f_{oxD})\frac{\partial f_{oxD}}{\partial x_D}$$

$$+\left\{\frac{\eta_R\,\eta_{oD}}{\Gamma(1-\alpha)t_R^\alpha}\frac{f_{oR}\ p_{cR}}{y_R^2}\int_0^{t_R t_D}(t_D-\ \xi_D)^{-\alpha}\left[\frac{\partial}{\partial\xi_D}\left(\frac{\partial p_{cD}}{\partial S_{wD}}\frac{\partial S_{wD}}{\partial y_D}\right)\right]d\xi_D\right\}(1-f_{oR}f_{oyD})\frac{\partial f_{oyD}}{\partial y_D}$$

$$+\left\{\frac{\eta_R\,\eta_{oD}+\ \eta_R\,\eta_{wD}}{\Gamma(1-\ \alpha)\,t_R^\alpha}\frac{f_{oR}\ p_{wR}}{y_R^2}\int_0^{t_R t_D}(t_D-\ \xi_D)^{-\alpha}\left[\frac{\partial^2 p_{wD}}{\partial\xi_D\partial y_D}\right]d\xi_D\right\}(1-f_{oR}f_{oyD})\frac{\partial f_{oyD}}{\partial y_D}$$

$$+\left\{\frac{\eta_R\,\eta_{oD}}{\Gamma(1-\alpha)t_R^\alpha}\frac{f_{oR}\ p_{cR}}{z_R^2}\int_0^{t_R t_D}(t_D-\ \xi_D)^{-\alpha}\left[\frac{\partial}{\partial\xi_D}\left(\frac{\partial p_{cD}}{\partial S_{wD}}\frac{\partial S_{wD}}{\partial z_D}\right)\right]d\xi_D\right\}(1-f_{oR}f_{ozD})\frac{\partial f_{ozD}}{\partial z_D}$$

$$+\left\{\frac{\eta_R\,\eta_{oD}+\ \eta_R\,\eta_{wD}}{\Gamma(1-\ \alpha)\,t_R^\alpha}\frac{f_{oR}\ p_{wR}}{z_R^2}\int_0^{t_R t_D}(t_D-\ \xi_D)^{-\alpha}\left[\frac{\partial^2 p_{wD}}{\partial\xi_D\partial z_D}\right]d\xi_D\right\}(1-f_{oR}f_{ozD})\frac{\partial f_{ozD}}{\partial z_D}$$

$$+(\rho_{oR}\,g_R\,z_R)\rho_{oD}\,g_D\,z_D+\left(\frac{\phi_R S_{wR}}{t_R}\right)\phi_D\frac{\partial S_{wD}}{\partial t_D}=0 \tag{25}$$

$$\left\{\int_0^{t_R t_D}(t_D-\ \xi_D)^{-\alpha}\left[\frac{\partial}{\partial\xi_D}\left(\frac{\partial p_{cD}}{\partial S_{wD}}\frac{\partial S_{wD}}{\partial x_D}\right)\right]d\xi_D\right\}(1-f_{oR}f_{oxD})\frac{\partial f_{oxD}}{\partial x_D}$$

$$+\left(\frac{p_{wR}}{p_{cR}}\right)\left\{\frac{\eta_{oD}+\eta_{wD}}{\eta_{oD}}\int_0^{t_R t_D}(t_D-\ \xi_D)^{-\alpha}\left[\frac{\partial^2 p_{wD}}{\partial\xi_D\partial x_D}\right]d\xi_D\right\}(1-f_{oR}f_{oxD})\frac{\partial f_{oxD}}{\partial x_D}$$

$$+\left(\frac{x_R^2}{y_R^2}\right)\left\{\int_0^{t_R t_D}(t_D-\ \xi_D)^{-\alpha}\left[\frac{\partial}{\partial\xi_D}\left(\frac{\partial p_{cD}}{\partial S_{wD}}\frac{\partial S_{wD}}{\partial y_D}\right)\right]d\xi_D\right\}(1-f_{oR}f_{oyD})\frac{\partial f_{oyD}}{\partial y_D}$$

$$+\left(\frac{x_R^2\,p_{wR}}{y_R^2\,p_{cR}}\right)\left\{\frac{\eta_{oD}+\eta_{wD}}{\eta_{oD}}\int_0^{t_R t_D}(t_D-\ \xi_D)^{-\alpha}\left[\frac{\partial^2 p_{wD}}{\partial\xi_D\partial y_D}\right]d\xi_D\right\}(1-f_{oR}f_{oyD})\frac{\partial f_{oyD}}{\partial y_D}$$

$$+\left(\frac{x_R^2}{z_R^2}\right)\left\{\int_0^{t_R t_D}(t_D-\ \xi_D)^{-\alpha}\left[\frac{\partial}{\partial\xi_D}\left(\frac{\partial p_{cD}}{\partial S_{wD}}\frac{\partial S_{wD}}{\partial z_D}\right)\right]d\xi_D\right\}(1-f_{oR}f_{ozD})\frac{\partial f_{ozD}}{\partial z_D}$$

$$+\left(\frac{x_R^2\,p_{wR}}{z_R^2\,p_{cR}}\right)\left\{\frac{\eta_{oD}+\eta_{wD}}{\eta_{oD}}\int_0^{t_R t_D}(t_D-\ \xi_D)^{-\alpha}\left[\frac{\partial^2 p_{wD}}{\partial\xi_D\partial z_D}\right]d\xi_D\right\}(1-f_{oR}f_{ozD})\frac{\partial f_{ozD}}{\partial z_D}$$

$$+\left[\frac{\rho_{oR}\ g_R\ z_R\ x_R^2\ t_R^{\alpha}\ \Gamma(1-\alpha)}{f_{oR}\ \eta_R\ p_{cR}}\right]\frac{\rho_{oD}\ g_D\ z_D}{\eta_{oD}}+\left[\frac{\phi_R S_{wR}\ x_R^2\ t_R^{\alpha-1}\ \Gamma(1-\alpha)}{f_{oR}\ \eta_R\ p_{cR}}\right]\frac{\phi_D}{\eta_{oD}}\frac{\partial S_{wD}}{\partial t_D}=0 \quad (26)$$

Table 2. Dimensionless constitutive relationship and constraints

Constitutive relationship and constraints
1. $\rho_{iD}(p_{iD})\ i=o,w$
2. $\eta_{iD}(k_{iD},\mu_{iD},p_{iD})\ i=o,w$
3. $(\phi_R)\phi_D \cong$ constant
4. $S_{oD}+\left(\frac{S_{wi}}{S_{wR}}\right)S_{wD}=1$
5. $\left(\frac{p_{oR}}{p_{cR}}\right)p_{oD}-\left(\frac{p_{wR}}{p_{cR}}\right)p_{wD}=p_{cD}$

Now, capillary pressure p_c may be expressed by the $J(S)$ function as

$$J(S)=\frac{p_c\sqrt{k}}{\sigma\cos\theta\sqrt{\phi}} \quad (27)$$

$$p_c=\frac{J(S)\,\sigma\cos\theta\sqrt{\phi}}{\sqrt{k}}$$

Differentiating both sides with respect to S_w

$$\frac{\partial p_c}{\partial S_w}=\frac{\sigma\cos\theta\sqrt{\phi}}{\sqrt{k}}\frac{\partial J(S)}{\partial S_w}$$

$$\frac{\partial p_{cD}}{\partial S_{wD}}=\left(\frac{J_R(S)\,\sigma_R\cos\theta_R\sqrt{\phi_R}}{p_{cR}\sqrt{k_R}}\right)\frac{J_D(S)\,\sigma_D\cos\theta_D\sqrt{\phi_D}}{\sqrt{k_D}}\frac{\partial J_D(S)}{\partial S_{wD}} \quad (28)$$

INITIAL AND BOUNDARY CONDITIONS

Initial condition:

$p(x,0)=p_i\ in\ dimensionless\ form\ as\ \left(\frac{p_R}{p_i}\right)p_D(i_D,0)=1, i=x,y,z$ (29)

Boundary condition: The external boundary is considered as no flow boundary i.e. closed reservoir. The interior boundary is considered as a constant production rate boundary.

1. *outer boundary:*
   According to Darcy's law:
   $u_{x=L}=-\frac{k}{\mu}\frac{\partial p}{\partial x}=0,\text{in dimensionless form,}\left.\frac{\partial p_D}{\partial x_D}\right]_{x_{iD}=x_i/L=1}=0$ (30)
2. *inner boundary:*
   According to Darcy's law, $q_{x=0}=Au_x=-\frac{kA_{yz}}{\mu}\frac{\partial p}{\partial x}$ in dimensionless form:

$$q_D q_R = -\left(\frac{k_R k_D A_{yzR} A_{yzD}}{\mu_R \mu_D}\right)\left(\frac{p_R}{x_R}\frac{\partial p_D}{\partial x_D}\right),$$
$$q_D = -\left(\frac{k_R\, p_R\, A_{yzR}}{q_R\, \mu_R\, i_R}\right)\left(\frac{k_D\, A_{yzD}}{\mu_D}\frac{\partial p_D}{\partial x_D}\right), \text{ where } i = L, H, W. \quad (31)$$

DERIVATION OF SCALING CRITERIA

Inspectional Analysis

Inspectional analysis requires the variables in a set of equations which fully describe the process. To derive the scaling groups by inspectional analysis the governing partial differential equations (Eqs. 3-4, 7-8, 18), initial and boundary conditions (Eqs. 29-31), constitutive relationships and constraints (Eqs. 9-11, Table 1) were formulated. These equations were then rewritten in terms of dimensionless variables and some constant characteristic reference quantities (Eqs. 19-28). The dimensionless constitutive relationships and constraints are presented in Table 2. The dimensionless form of initial and boundary conditions are presented in (Eqs. 29-31). Finally, various similarity groups were identified. Table 3 lists the similarity groups derived from inspectional analysis.

Table 3. Similarity groups from inspectional analysis

$sg_1 = \frac{L^2}{H^2}$	$sg_7 = \frac{S_{wi}}{S_{wR}}$	$sg_{13} = \frac{u_{wzR}}{U_R}$	$sg_{19} = \frac{u_{wzR}}{U_R\, f_{wR}}$	$sg_{25} = \frac{\rho_o}{\rho_w}$
$sg_2 = \frac{L^2}{W^2}$	$sg_8 = \frac{u_{oxR}}{U_R}$	$sg_{14} = \frac{u_{oxR}}{U_R\, f_{oR}}$	$sg_{20} = \frac{L^2}{W^2}\frac{p_{wR}}{p_{cR}}$	$sg_{26} = f_{oR}$
$sg_3 = \frac{p_{oR}}{p_{cR}}$	$sg_9 = \frac{u_{wxR}}{U_R}$	$sg_{15} = \frac{u_{oyR}}{U_R\, f_{oR}}$	$sg_{21} = \frac{L^2}{H^2}\frac{p_{wR}}{p_{cR}}$	$sg_{27} = \phi_R$
$sg_4 = \frac{p_R}{p_i}$	$sg_{10} = \frac{u_{oyR}}{U_R}$	$sg_{16} = \frac{u_{ozR}}{U_R\, f_{oR}}$	$sg_{22} = \frac{k_R\, p_R\, A_{yzR}}{q_R\, \mu_R\, L}$	$sg_{28} = \frac{J_R(S)\, \sigma_R \cos\theta_R \sqrt{\phi_R}}{p_{cR}\sqrt{k_R}}$
$sg_5 = \frac{p_{wR}}{p_{cR}}$	$sg_{11} = \frac{u_{wyR}}{U_R}$	$sg_{17} = \frac{u_{wxR}}{U_R\, f_{wR}}$	$sg_{23} = \frac{k_R\, p_R\, A_{yzR}}{q_R\, \mu_R\, H}$	$sg_{29} = \frac{\phi_R\, S_{wR}\, L^2\, t_R^{\alpha-1}\,\Gamma(1-\alpha)}{f_{oR}\, \eta_R\, p_{cR}}$
$sg_6 = \frac{S_{oi}}{S_{wR}}$	$sg_{12} = \frac{u_{ozR}}{U_R}$	$sg_{18} = \frac{u_{wyR}}{U_R\, f_{wR}}$	$sg_{24} = \frac{k_R\, p_R\, A_{yzR}}{q_R\, \mu_R\, W}$	$sg_{30} = \frac{\rho_{oR}\, g_R\, H\, L^2\, t_R^{\alpha}\,\Gamma(1-\alpha)}{f_{oR}\, \eta_R\, p_{cR}}$

Scaling Criteria

The scaling requirement for this process can be stated as follows;

- These similarity groups in Table 3 should be similar both in model and prototype
- The dimensionless form of initial and boundary conditions must be same
- The constitutive relationships and constraints must be the same for model and prototype also

- *J(S)* must be the same functions of the dimensionless saturation, S_w.

Development of Relaxed Criteria

Based on the assumptions in the approach 1, the terms corresponding to these assumptions (the terms that does not scale by the approach) are eliminated from the governing equation shown in Eq. (25). Each term is then divided by one of the remaining coefficients to yield the dimensionless form of equation. The coefficients represent the relaxed set of similarity groups which can then be reduced to their simplest form. The constitutive relationships, constraints, and initial and boundary conditions are treated in a similar manner. For Approach 1, the effects of gravity are assumed negligible. For Approach 2, the effects the vertical pressure gradient due to viscous and capillary forces is negligible. For Approach 3, the effects of saturation, permeability, memory, the saturation pressure-saturation temperature relationship and capillary forces are not scaled. For Approach 4, the effects capillary forces are not scaled.

Approach 1. Same Porous Medium, Same Fluids, Same Pressure Drop, Same Temperature and Geometric Similarity

In this process, initial pressure and temperature as well as the maximum pressure and temperature change must be same in the model and prototype. In addition, using the same porous media (same porosity, same permeability, same grain size and same wettability) would allow better scaling of the irreducible saturations and relative permeabilities. In our case, fluid memory related to formation can be scaled properly and fluid memory related to formation fluid can also be scaled properly due to same porous fluid. The main advantage of this approach is to scale the properties such as viscosity, density, fluid memory and equilibrium constants, which depend on pressure, temperature and composition of formation, are more accurately scaled. Therefore, this approach would insure that viscous forces, capillary forces, and diffusive forces are properly scaled while maintaining geometric similarity. However, it does not allow the scaling of gravitational and dispersive effects. The relaxed sets of scaling criteria for the approach are listed in Table 4. Here $x_R = y_R = z_R = L$.

In addition of these scaling groups, all the dimensionless properties (Table 2) must be the same function of their dimensionless variables for the prototype and model. For a model reduced in length by a scaling factor “a” and employing the same fluids as the prototype:

Here, $a = \frac{L_{proto\ \ type}}{L_{model}}$ and

- $\Delta p_{max}\,(p_{max} - p_{min})$, p_{oi}, $p_{production}$,T, k, S_{oi}, S_{wi}, η_R must be the same in model and prototype
- H, W, q must be reduced by “a” from prototype to model
- t will be reduced by $a^{2/(\alpha-1)}$ from prototype to model

Approach 2. Same Porous Medium, Same Fluids, Same Pressure Drop, Same Temperature and Relaxed Geometric Similarity

Table 4. Relaxed sets of similarity groups by Approach 1

$sg_1 = \frac{L^2}{H^2}$	$sg_7 = \frac{S_{wi}}{S_{wR}}$	$sg_{13} = \frac{u_{wzR}}{U_R}$	$sg_{19} = \frac{u_{wzR}}{U_R\, f_{wR}}$	$sg_{24} = \frac{k_R\, p_R\, A_{yzR}}{q_R\, \mu_R\, W}$
$sg_2 = \frac{L^2}{W^2}$	$sg_8 = \frac{u_{oxR}}{U_R}$	$sg_{14} = \frac{u_{oxR}}{U_R\, f_{oR}}$	$sg_{20} = \frac{L^2}{W^2}\frac{p_{wR}}{p_{cR}}$	$sg_{25} = \frac{\rho_o}{\rho_w}$
$sg_3 = \frac{p_{oR}}{p_{cR}}$	$sg_9 = \frac{u_{wxR}}{U_R}$	$sg_{15} = \frac{u_{oyR}}{U_R\, f_{oR}}$	$sg_{21} = \frac{L^2}{H^2}\frac{p_{wR}}{p_{cR}}$	$sg_{26} = f_{oR}$
				$sg_{27} = \phi_R$
$sg_4 = \frac{p_R}{p_i}$	$sg_{10} = \frac{u_{oyR}}{U_R}$	$sg_{16} = \frac{u_{ozR}}{U_R\, f_{oR}}$	$sg_{22} = \frac{k_R\, p_R\, A_{yzR}}{q_R\, \mu_R\, L}$	$sg_{28} = \frac{J_R(S)\, \sigma_R \cos\theta_R \sqrt{\phi_R}}{p_{cR}\sqrt{k_R}}$
$sg_5 = \frac{p_{wR}}{p_{cR}}$	$sg_{11} = \frac{u_{wyR}}{U_R}$	$sg_{17} = \frac{u_{wxR}}{U_R\, f_{wR}}$	$sg_{23} = \frac{k_R\, p_R\, A_{yzR}}{q_R\, \mu_R\, H}$	$sg_{29} = \frac{\phi_R\, S_{wR}\, L^2\, t_R^{\alpha-1}\, \Gamma(1-\alpha)}{f_{oR}\, \eta_R\, p_{cR}}$
	$sg_{12} = \frac{u_{ozR}}{U_R}$	$sg_{18} = \frac{u_{wyR}}{U_R\, f_{wR}}$		
$sg_6 = \frac{S_{oi}}{S_{wR}}$				

To combine the advantages of using the same fluids, the same porous medium and similar pressure and temperature conditions with proper scaling of the gravitational effects, the requirement of geometric similarity must be relaxed. If geometric similarity is relaxed and if the vertical pressure gradient due to viscous and capillary forces is small, the viscous and gravitational forces may be scaled for the case of horizontal reservoirs. The relaxed requirements for this approach are listed in Table 5. The most significant difference is the choice of the reference quantity for the vertical coordinate z_R. It is now $z_R^2 = (L^2\, p_{wR}/p_{cR})$.

In addition of these scaling groups, all the dimensionless properties (Table 2) must be the same function of their dimensionless variables for the prototype and model. For a model reduced in length by a scaling factor "a" and employing the same fluids as the prototype:

- $\Delta p_{max}\,(p_{max} - p_{min})$, p_{oi}, $p_{production}$,T, k, S_{oi}, S_{wi}, η_R must be the same in model and prototype
- $H, W,$ must be reduced by "a" from prototype to model
- q must be increased by "a" from prototype to model
- the reservoir must be horizontal

t will be reduced by $a^{-2/(\alpha-1)}$ from prototype to model

In order to satisfy the scaling groups related to this approach, geometric similarity, viscous forces, and gravitational forces are satisfied. Therefore, different porous medium, and different pressure drops are necessary between model and prototype. The disadvantage of this approach is that it can not properly scale the related groups of saturation, permeability and memory. This approach violates some of the requirements of the constitutive relationships, constraints and boundary conditions. This method cannot scale the saturation pressure-saturation temperature relationship for hot water. This leads to an improper match of the boundary conditions. Water density and other properties which depend on pressure will not be properly scaled either. The effects of capillary forces are not scaled. For the calculation of *t*, capillary pressure is considered negligible. The relaxed requirements for this approach are listed in Table 6.

Table 5. Relaxed sets of similarity groups by Approach 2

$sg_2 = \frac{L^2}{W^2}$	$sg_7 = \frac{S_{wi}}{S_{wR}}$	$sg_{14} = \frac{u_{oxR}}{U_R f_{oR}}$	$sg_{22} = \frac{k_R p_R p_{wR} W}{q_R \mu_R \; p_{cR} L^2}$	$sg_{28} = \frac{J_R(S) \sigma_R \cos\theta_R \sqrt{\phi_R}}{p_{cR}\sqrt{k_R}}$
$sg_3 = \frac{p_{oR}}{p_{cR}}$	$sg_8 = \frac{u_{oxR}}{U_R}$	$sg_{15} = \frac{u_{oyR}}{U_R f_{oR}}$	$sg_{24} = \frac{k_R p_R p_{wR} L^2}{p_{cR} q_R \mu_R}$	$sg_{29} = \frac{\phi_R S_{wR} L^2 t_R^{\alpha-1} \Gamma(1-\alpha)}{f_{oR} \eta_R p_{cR}}$
$sg_4 = \frac{p_R}{p_i}$	$sg_9 = \frac{u_{wxR}}{U_R}$	$sg_{17} = \frac{u_{wxR}}{U_R f_{wR}}$	$sg_{25} = \frac{\rho_o}{\rho_w}$	$sg_{30} = \frac{p_{wR} \rho_{oR} g_R L^4 t_R^{\alpha} \Gamma(1-\alpha)}{f_{oR} \eta_R p_{cR}^2}$
$sg_5 = \frac{p_{wR}}{p_{cR}}$	$sg_{10} = \frac{u_{oyR}}{U_R}$	$sg_{18} = \frac{u_{wyR}}{U_R f_{wR}}$	$sg_{26} = f_{oR}$	
$sg_6 = \frac{S_{oi}}{S_{wR}}$	$sg_{11} = \frac{u_{wyR}}{U_R}$	$sg_{20} = \frac{L^2}{W^2}\frac{p_{wR}}{p_{cR}}$	$sg_{27} = \phi_R$	

Approach 3. Different Porous Medium, Same Fluids, Same Temperature, Different Pressure Drop, and Geometric Similarity

Table 6. Relaxed sets of similarity groups by Approach 3

$sg_1 = \frac{L^2}{H^2}$	$sg_4 = \frac{p_R}{p_i}$	$sg_{20} = \frac{L^2}{W^2}\frac{p_{wR}}{p_{cR}}$	$sg_{23} = \frac{k_R p_R A_{yzR}}{q_R \mu_R H}$	$sg_{27} = \phi_R$
$sg_2 = \frac{L^2}{W^2}$	$sg_5 = \frac{p_{wR}}{p_{cR}}$	$sg_{21} = \frac{L^2}{H^2}\frac{p_{wR}}{p_{cR}}$	$sg_{24} = \frac{k_R p_R A_{yzR}}{q_R \mu_R W}$	$sg_{28} = \frac{J_R(S) \sigma_R \cos\theta_R \sqrt{\phi_R}}{p_{cR}\sqrt{k_R}}$
$sg_3 = \frac{p_{oR}}{p_{cR}}$	$sg_6 = \frac{S_{oi}}{S_{wR}}$	$sg_{22} = \frac{k_R p_R A_{yzR}}{q_R \mu_R L}$	$sg_{25} = \frac{\rho_o}{\rho_w}$	$sg_{29} = \frac{\phi_R S_{wR}}{t_R \rho_{oR} g_R W}$
			$sg_{26} = f_{oR}$	$sg_{30} = \frac{\rho_{oR} g_R H L^2 t_R^{\alpha} \Gamma(1-\alpha)}{f_{oR} \eta_R p_{cR}}$

In addition of these scaling groups, for a model reduced in length by a scaling factor “a” and employing the same fluids as the prototype:

- ϕ, S_{oi}, S_{wi}, must be the same in model and prototype
- H, W, must be reduced by “a” from prototype to model
- t will be reduced by $a^{-3/\alpha}$ from prototype to model

Approach 4. Different Porous Medium, Same Fluids, Same Temperature, Different Same Pressure Drop, and Relaxed Geometric Similarity

Relaxation of gravitational effects is the major shortcomings of approach 2. In this approach the viscous and gravitational forces are balanced which repeat many of the drawback of approach 3. This is done by relaxing pressure drop and requires different porous media. This approach cannot scale capillary pressure. The reference quantity for the vertical coordinate z_R is calculated by setting the ratio of vertical and length distance ratio equals one. It is now $z_R^2 = L^2$. The main disadvantage of this approach is that time is scaled up by the factor “a”. This indicates that experimental time is more than that of field. The relaxed requirements for this approach are listed in Table 7.

Table 7. Relaxed sets of similarity groups by Approach 4

$sg_1 = \frac{L^2}{H^2}$	$sg_7 = \frac{S_{wi}}{S_{wR}}$	$sg_{12} = \frac{u_{ozR}}{U_R}$	$sg_{17} = \frac{u_{wxR}}{U_R\, f_{wR}}$	$sg_{25} = \frac{\rho_o}{\rho_w}$
$sg_2 = \frac{L^2}{W^2}$	$sg_8 = \frac{u_{oxR}}{U_R}$	$sg_{13} = \frac{u_{wzR}}{U_R}$	$sg_{18} = \frac{u_{wyR}}{U_R\, f_{wR}}$	$sg_{26} = f_{oR}$
$sg_4 = \frac{p_R}{p_i}$	$sg_9 = \frac{u_{wxR}}{U_R}$	$sg_{14} = \frac{u_{oxR}}{U_R\, f_{oR}}$	$sg_{19} = \frac{u_{wzR}}{U_R\, f_{wR}}$	$sg_{27} = \phi_R$
$sg_6 = \frac{S_{oi}}{S_{wR}}$	$sg_{10} = \frac{u_{oyR}}{U_R}$	$sg_{15} = \frac{u_{oyR}}{U_R\, f_{oR}}$	$sg_{22} = \frac{k_R\, p_R\, A_{yzR}}{q_R\, \mu_R\, L}$	$sg_{29} = \frac{\phi_R\, S_{wR}\, L^2\, t_R^{\alpha-1}\, \Gamma(1-\alpha)}{f_{oR}\, \eta_R\, p_{wR}}$
	$sg_{11} = \frac{u_{wyR}}{U_R}$	$sg_{16} = \frac{u_{ozR}}{U_R\, f_{oR}}$	$sg_{23} = \frac{k_R\, p_R\, W}{q_R\, \mu_R}$	$sg_{30} = \frac{\rho_{oR}\, g_R\, H\, L^2\, t_R^{\alpha}\, \Gamma(1-\alpha)}{f_{oR}\, \eta_R\, p_{wR}}$

In addition of these scaling groups, for a model reduced in length by a scaling factor “a” and employing the same fluids as the prototype:

- $\phi, S_{oi},\ S_{wi}, \Gamma(1-\alpha), p_{wi},\ f_{oi}$ must be the same in model and prototype
- L, W must be reduced by “a” from prototype to model
- t will be reduced by a from prototype to model

Dimensional Analysis

Dimensional analysis requires the knowledge of the complete set of relevant variables influencing the process. The first step in the dimensional analysis of a problem must be to ascertain which variables are relevant to the problem.

Table 8. Complete variables in the process for dimensional analysis

Symbols	Dimensions	Symbols	Dimensions	Symbols	Dimensions
A_{yz}	$[L^2]$	q_i	$[M/L^2\ t\ ]$	u_{wy}	$[L/\ t\ ]$
k	$[L^2]$	t	$[t]$	u_{oz}	$[L/\ t\ ]$
L	$[L]$	u_i	$[L/\ t\ ]$	u_{wz}	$[L/\ t\ ]$
H	$[L]$	u_o	$[L/\ t\ ]$	ρ_o	$[M/L^3]$
W	$[L]$	u_x	$[L/\ t\ ]$	ρ_w	$[M/L^3]$
p	$[M/L\ t^2]$	g	$[L/\ t^2\ ]$	ξ	$[t]$
p_c	$[M/L\ t^2]$	u_w	$[L/\ t\ ]$	η	$[L^3\ t^{1+\alpha}/M]$
p_i	$[M/L\ t^2]$	U_x	$[L/\ t\ ]$	η_o	$[L^3\ t^{1+\alpha}/M]$
p_o	$[M/L\ t^2]$	u_{ox}	$[L/\ t\ ]$	η_w	$[L^3\ t^{1+\alpha}/M]$
p_w	$[M/L\ t^2]$	u_{wx}	$[L/\ t\ ]$	σ	$[M/t^2]$
q	$[M/L^2\ t\ ]$	u_{oy}	$[L/\ t\ ]$	μ	$[M/L\ t]$

Special care should be exercised at this stage that all the relevant variables are included. This analysis often yields a more complete set of similarity groups but the physical meaning of the similarity groups themselves is generally more apparent from inspectional analysis. Dimensional analysis is usually used in conjunction with inspectional analysis to ensure important groups are not omitted. The similarity groups may also be derived using dimensional analysis. After the relevant variables for the process are selected, the similarity groups can be determined using the Buckingham π-theorem. Table 8 lists the symbols, dimensions of the variables selected. Table 9 shows the similarity groups derived by this method. There are some more scaling groups identified by dimensional analysis. These are $\pi_1, \pi_{10}, \pi_{11}, \pi_{23}, \pi_{26}, \pi_{27}, \pi_{28}, \pi_{30}$.

RESULTS AND DISCUSSION

To find out the displacement efficiency of the application of different Approaches, pressure drop and time are considered as the principle criteria in the selection of scaling laws. When fluid memory is being encountered, it is necessary to select an appropriate Approach to scale the different parameters from lab to field or vice versa. In solving different similarity groups, $\alpha = 0.1 \ and \ 0.2, \phi = 0.3, S_w = 0.24, \eta = 0.343249, \rho_0 = 50.0 \ lb_m/ft^3$, $L = 1000.0 \ ft$, $W = 400.0 \ ft, H = 50.0 \ ft$, $p_c = 30.0 \ psi, g = 32.2 \ ft/s^2, f_0 = 0.2, p_i = 3000.0 \ psi$, and a pressure drop of $0 \sim 320 \ psi$ have been regarded.

Approach 1

Equating the similarity groups Group 3 and Group 29 becomes;

$$sg_3 = sg_{29} \Rightarrow \frac{p_{oR}}{p_{cR}} = \frac{\phi_R \, S_{wR} \, L^2 \, t_R^{\alpha-1} \, \Gamma(1-\alpha)}{f_{oR} \, \eta_R \, p_{cR}}$$

$$p_{oR} = \frac{\phi_R \, S_{wR} \, L^2 \, t_R^{\alpha-1} \, \Gamma(1-\alpha)}{f_{oR} \, \eta_R}$$

$$t_R^{\alpha-1} = \frac{f_{oR} \, \eta_R \, p_{oR}}{\phi_R \, S_{wR} \, L^2 \, \Gamma(1-\alpha)}$$

$$t_R = \left[\frac{f_{oR} \, \eta_R \, p_{oR}}{\phi_R \, S_{wR} \, L^2 \, \Gamma(1-\alpha)}\right]^{1/(\alpha-1)} \quad (32)$$

Figure 1 shows the variation of pressure drop with time for different fraction derivative, α, values when Approach 1 is considered. Equation (32) is used in developing this plotting. The graph shows that pressure drop decreases with time from a reference point which has a non-linear trend. There is a huge pressure drop at the beginning of oil-water displacement process.

This gap gradually decreases with time. Moreover, α has a great role in displacement process. When α increases pressure drop delays during the process. This simply means that oil displacement would be more and swift efficiency of the process will increase when memory of the fluid is encountered. However, it is more interesting that there would be no early water break-through in the production well. The viscous fingering effects of the EOR process would also be less pronounced during the oil-water interaction in the formation if memory concept is used.

Table 9. Similarity groups from dimensional analysis

Scaling Group	Description	Symbols	Dimensions
$\pi_1 = [A_{yz}/L^2]$	geometric factor	$\pi_{20} = [u_{wy}/ U_x]$	ratio of water velocity in y-direction to total fluid velocity
$\pi_2 = [H/L]$	geometric factor	$\pi_{21} = [u_{oz}/ U_x]$	ratio of oil velocity in z-direction to total fluid velocity
$\pi_3 = [W/L]$	geometric factor	$\pi_{22} = [u_{wz}/ U_x]$	ratio of water velocity in z-direction to total fluid velocity
$\pi_4 = [k/L^2]$	ratio of permeability to system dimensions	$\pi_{23} = [g\,L/ U_x^2]$	
$\pi_5 = [p/\rho_w\, U_x^2]$	ratio of viscous to gravity forces	$\pi_{24} = [\rho_o/\rho_w]$	density factor for oil
$\pi_6 = [p_c/\rho_w\, U_x^2]$	ratio of capillary to gravity forces	$\pi_{25} = [U_x\, \xi/L]$	
$\pi_7 = [p_i/\rho_w\, U_x^2]$	ratio of viscous to gravity forces	$\pi_{26} = [\rho_w\, \eta\, U_x^{1+\alpha}/L^{1+\alpha}]$	ratio of gravity to fluid movement with memory forces
$\pi_8 = [p_o/\rho_w\, U_x^2]$	ratio of viscous to gravity forces for oil	$\pi_{27} = [\rho_w\, \eta_o\, U_x^{1+\alpha}/L^{1+\alpha}]$	ratio of gravity to fluid movement with memory forces for oil
$\pi_9 = [p_w/\rho_w\, U_x^2]$	ratio of viscous to gravity forces for water	$\pi_{28} = [\rho_w\, \eta_w\, U_x^{1+\alpha}/L^{1+\alpha}]$	ratio of gravity to fluid movement with memory forces for water
$\pi_{10} = [q/\rho_w\, U_x]$	ratio of mass flow rate to gravity force	$\pi_{29} = [\sigma/\rho_w\, U_x^2\, L]$	ratio of capillary to gravity forces
$\pi_{11} = [q_i/\rho_w\, U_x]$	ratio of initial mass flow rate to gravity force	$\pi_{30} = [\mu/\rho_w\, U_x\, L]$	ratio of viscous to gravity forces
$\pi_{12} = [u_i/ U_x]$	ratio of initial velocity to slip velocity	$\pi_{31} = [S_o]$	oil saturation factor
$\pi_{13} = [u_o/ U_x]$	ratio of oil velocity to total fluid velocity	$\pi_{32} = [S_w]$	water saturation factor
$\pi_{14} = [u_x/ U_x]$	ratio of velocity in x-direction to total fluid velocity	$\pi_{33} = [f_o]$	velocity factor for oil
$\pi_{15} = [u_w/ U_x]$	ratio of water velocity to total fluid velocity	$\pi_{34} = [f_w]$	velocity factor for water
$\pi_{16} = [U_x\, t/ L]$	distance travel ratio	$\pi_{35} = [J(S)]$	J-function
$\pi_{17} = [u_{ox}/ U_x]$	ratio of oil velocity in x-direction to total fluid velocity	$\pi_{36} = [\phi]$	porosity factor
$\pi_{18} = [u_{wx}/ U_x]$	ratio of water velocity in x-direction to total fluid velocity	$\pi_{37} = [\alpha]$	Fractional order factor
$\pi_{19} = [u_{oy}/ U_x]$	ratio of oil velocity in y-direction to total fluid velocity		

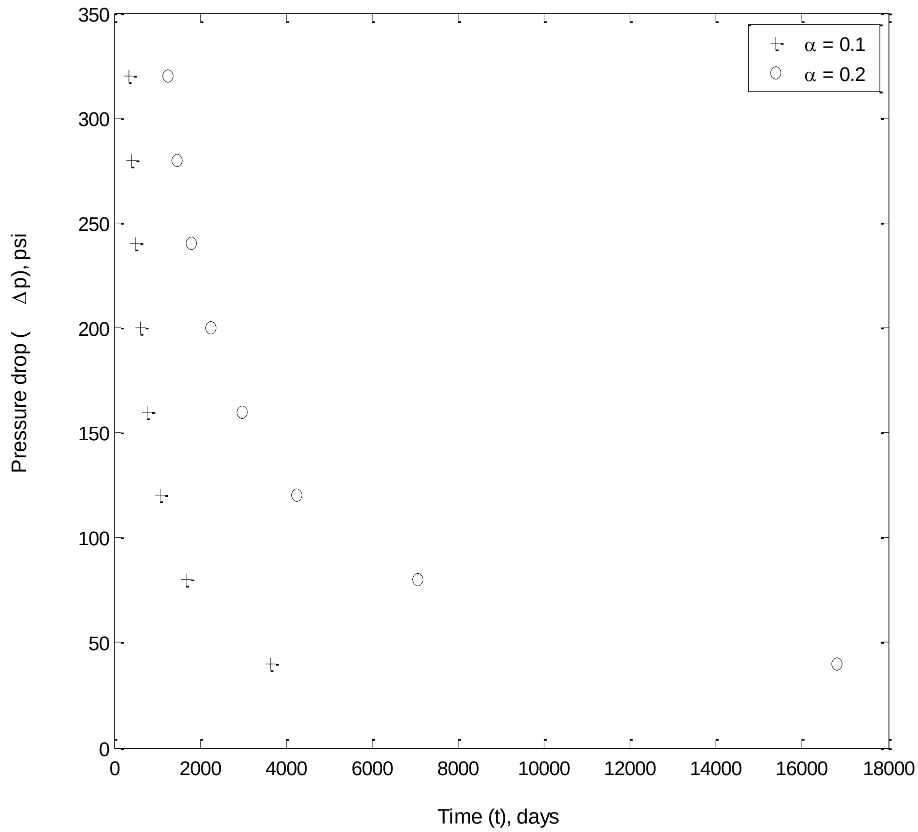

Figure 1. Variation of pressure drop with time for Approach 1.

Approach 2

Equating the similarity groups Group 20 and Group 29 becomes;

$$sg_{21} = sg_{29} \Rightarrow \frac{L^2}{W^2}\frac{p_{wR}}{p_{cR}} = \frac{\phi_R\, S_{wR}\, L^2\, t_R^{\alpha-1}\, \Gamma(1-\alpha)}{f_{oR}\, \eta_R\, p_{cR}}$$

$$t_R^{\alpha-1} = \frac{p_{wR}\, f_{oR}\, \eta_R}{W^2 \phi_R\, S_{wR}\, \Gamma(1-\alpha)}$$

$$t_R = \left[\frac{p_{wR}\, f_{oR}\, \eta_R}{W^2 \phi_R\, S_{wR}\, \Gamma(1-\alpha)}\right]^{1/(\alpha-1)} \tag{33}$$

Figure 2 shows the variation of pressure drop vs. time for different α values when Approach 2 is considered. Equation (33) is used in developing this plotting. The trend and nature of the graph is same as explained for Approach 1 except the time duration of the process. When Approach 2 is used, it takes less time to complete the displacement process comparing with Approach 1.

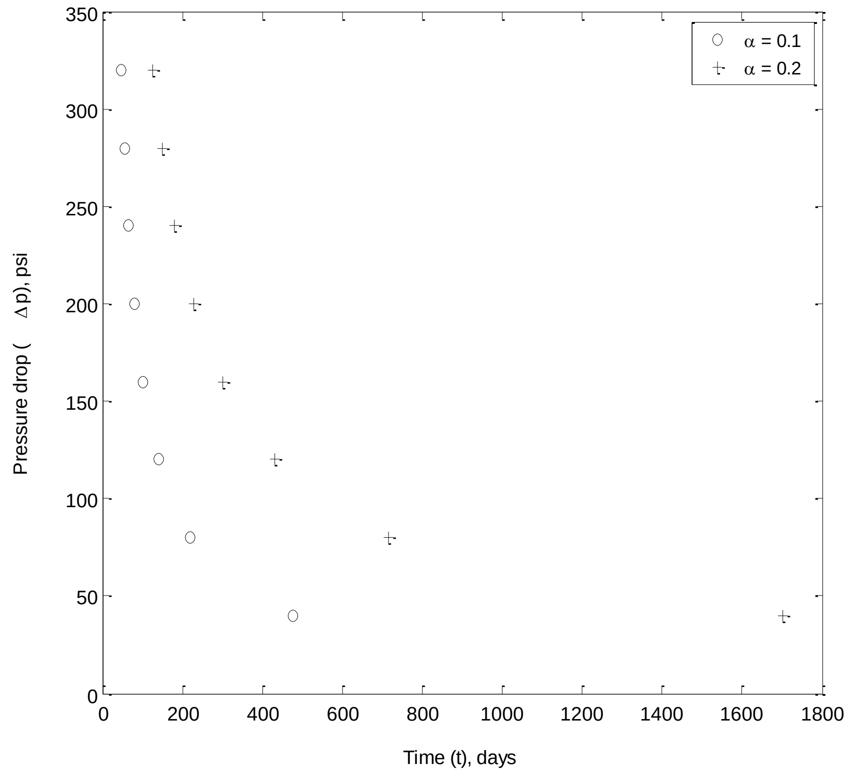

Figure 2. Variation of pressure drop with time for Approach 2.

Approach 3

Equating the similarity groups Group 21 and Group 29 becomes;

$$sg_{21} = sg_{29} \Rightarrow \frac{L^2}{H^2}\frac{p_{wR}}{p_{cR}} = \frac{\phi_R\, S_{wR}}{t_R\, \rho_{oR}\, g_R\, W}$$

$$t_R = \frac{\phi_R\, S_{wR}\, H^2\, p_{cR}}{\rho_{oR}\, g_R\, W\, L^2\, p_{wR}} \tag{34}$$

Figure 3 shows the variation of pressure drop with time for different α values when Approach 3 is considered. Equation (34) is used in developing this plotting. The graph shows that pressure drop increases with time from a reference point. It should be noted that there is no memory effects in this Approach. Here, the time domain is very short during the displacement process and pressure drop varies linearly with time.

This Approach indicates that, if memory effect is ignored, oil displacement would not be more and swift efficiency of the process will be lesser than that of Approaches based on memory. Moreover, early water break-through in the production well will be traced and viscous fingering effects of the EOR process will be stronger than that of memory based Approaches.

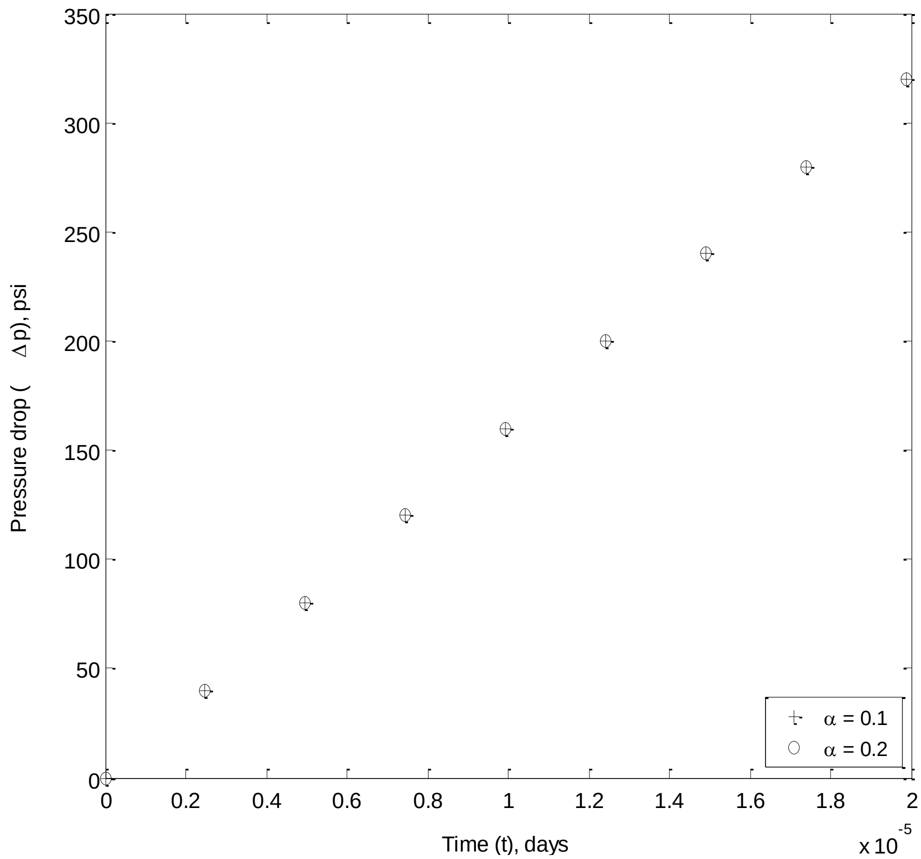

Figure 3. Variation of pressure drop with time for Approach 3.

Approach 4

Equating the similarity groups Group 25 and Group 29 becomes;

$$sg_{25} = sg_{29} \Rightarrow \frac{\rho_o}{\rho_w} = \frac{\phi_R \, S_{wR} \, L^2 \, t_R^{\alpha-1} \, \Gamma(1-\alpha)}{f_{oR} \, \eta_R \, p_{wR}}$$

$$t_R^{\alpha-1} = \frac{\rho_o \, f_{oR} \, \eta_R \, p_{wR}}{\rho_w \, \phi_R \, S_{wR} \, L^2 \, \Gamma(1-\alpha)}$$

$$t_R = \left[\frac{\rho_o \, f_{oR} \, \eta_R \, p_{wR}}{\rho_w \, \phi_R \, S_{wR} \, L^2 \, \Gamma(1-\alpha)}\right]^{1/(\alpha-1)} \tag{35}$$

Figure 4 shows the variation of pressure drop vs. time for different α values when Approach 4 is considered. Equation (35) is used in developing this plotting. The trend and nature of the graph is same as explained for Approach 1 and 2 except the time duration of the process. When Approach 4 is used, it takes more time to complete the displacement process comparing with Approach 1 and 2.

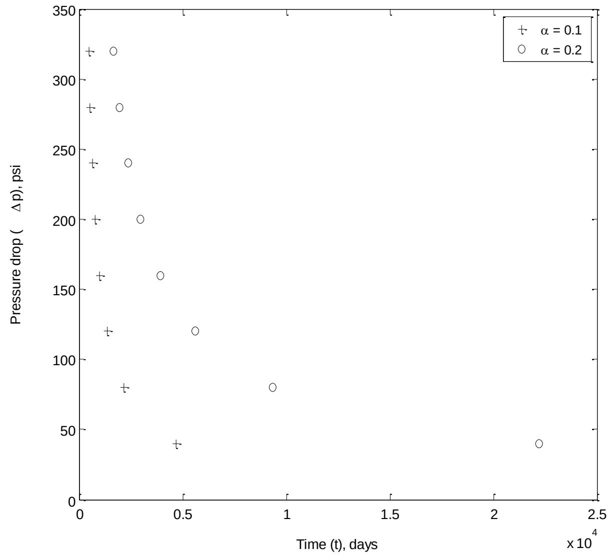

Figure 4. Variation of pressure drop with time for Approach 4.

Comparison of Different Approaches

Figure 5 shows the variation of pressure drop with time for different Approaches when $\alpha = 0.1$. A comparison of different Approaches is depicted in this figure. Approach 4 shows the more efficient in the oil-water displacement process when memory is taken care as a function of time.

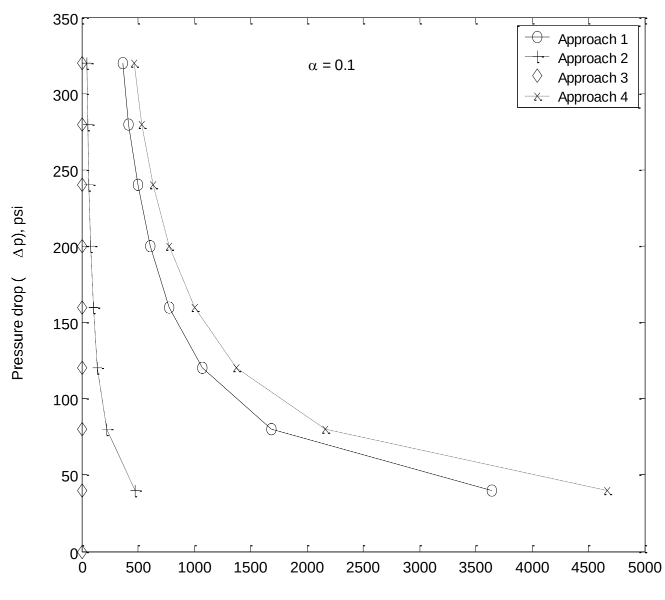

Figure 5. Variation of pressure drop with time for different Approaches.

Approach 1 is also efficient comparing with Approaches 2 and 3. The use of Approach 3 does not give any significant information during the process when memory of the fluid is disregarded. It is better to use Approach 4 or Approach 1 in the case of memory reflection.

CONCLUSIONS

This paper introduces new scaling criteria for oil-water displacement based on the implementation of memory concept. Relaxed sets of similarity groups and a complete set of similarity groups have also been identified. An efficient Approach is outlined for oil-water displacement process with memory. The choice of a subset is considered based on uniform porosities, pressure drop and geometrical similarities. The subset of the dimensionless groups neglected the effect of dispersive forces. However, future scaled up experimental studies will provide a deeper insight into the fluid-fluid interactions at a scaled up level and this paper may be a guidance to reduce considerable expenditures associated with oil-water displacement process in an EOR scheme. In future, the lab experimental results based on memory concept can be used to predict field performance in petroleum industry.

ACKNOWLEDGMENTS

The authors would like to thank the Atlantic Canada Opportunities Agency (ACOA) for funding this project under the Atlantic Innovation Fund (AIF). The first author would also like to thank Natural Sciences and Engineering Research Council of Canada (NSERC) for funding.

REFERENCES

Bansal, A. and Islam, M.R. 1994. Scaled Model Studies of Heavy Oil Recovery from an Alaskan Reservoir Using Gravity-assisted Gas Injection. *J of Canadian Petroleum Technology*. 33 (6): 52 – 61, June.

Basu, A. and Islam, M.R. 2007. Scaling up of Chemical Injection Experiments. *Petroleum Science and Technology*, in press.

Coskuner, G. and Bentsen, R.G. 1988. Hele Shaw Cell Study of a new approach to instability theory in porous media. *J. of Canadian Petroleum Technology*. 27(1): 87 – 95.

Farouq Ali, S.M. and Redford, D.A. 1977. Physical Modeling of In Situ Recovery Methods for Oil *Sands. Oil Sands*. 319 – 325.

Farouq Ali, S.M., Redford, D.A. and Islam, M.R. 1987. Scaling Laws for Enhanced Oil Recovery Experiments. China-Canada Joint Technical Conference on Heavy Oil Recovery. Zhou Zhou City, China.

Geertsma, J., Croes, G.A., and Schwarz. 1956. Theory of Dimensionally Scaled Models of Petroleum Reservoirs. *Petroleum Trans*., AIME, 207: 118 – 127.

Hossain, M. E., Ketata, C., and Islam, M. R. 2009a. A Scaled Model Study of Waterjet Drilling. *Petroleum Science and Technology*, 27, pp. 1261 – 1273.

Hossain, M. E., Mousavizadegan, S. H. and Islam, M. R. 2009b. Effects of Memory on the Complex Rock-Fluid Properties of a Reservoir Stress-Strain Model. *Petroleum Science and Technology*, 27 (10), pp. 1109 – 1123.

Hossain, M E., Mousavizadegan, S. H. and Islam, M. R. 2008. A Novel Fluid Flow Model with Memory for Porous Media Applications. MTDM Conference 2008, Mechanics of Time Dependent Materials Conference, March 30 - April 4, 2008, Monterey, California.

Hossain, M. E., Mousavizadegan, S. H. and Islam, M. R. 2007. A Novel Memory Based Stress-Strain Model for Reservoir Characterization. *Journal Nature Science and Sustainable Technology*, Volume 1(4), pp. 653 – 678.

Islam, M.R. 1987. Mobility Control in Waterflooding Oil Reservoirs with a Bottom- Water Zone. PhD dissertation, Department of Mining, Metallurgical and Petroleum Engineering, U of Alberta, Edmonton, Alberta, Canada.

Islam, M.R. and Farouq Ali, S.M. 1990. New Scaling Criteria for Chemical Flooding Experiments. *J. of Canadian Petroleum Technology*, 29 (1): 29 – 36, January – February.

Islam, M.R. and Farouq Ali, S.M. 1992. New Scaling Criteria for Chemical Flooding Experiments. *J. of Petroleum Science and Engineering*. 6: 367 – 379.

Islam, M.R. Chakma, A. and Jha, K.N. 1994. Heavy Oil Recovery by Inert Gas Injection with Horizontal Wells. *J. of Petroleum Science and Engineering*. 11: 213 – 226.

Kimber, K.D., Farouq Ali, S.M. and Puttagunta, V.R. 1988. New Scaling Criteria and their Relative merits for Steam Recovery Experiments. *J. of Canadian Petroleum Technology*, 27 (4): 86 – 94, July – August.

Loomis, A.G, and Crowell, D.G. 1964. Theory and Application of Dimensional and Inspectional Analysis to Model Study of Fluid Displacements in Petroleum Reservoirs. Bureau of Mines Report, R 6546, March.

Lozada, D. and Farouq Ali, S.M. 1987. New Scaling Criteria for Partial Equilibrium Immiscible Carbon Dioxide Drive. Paper no – 87-38-23, presented in 38th Annual Technical Meeting of the Petroleum Society of CIM, Calgary, Canada, June 7 – 10, 393 – 410.

Lozada, D. and Farouq Ali, S.M. 1988. Experimental Design for Non-Equilibrium Immiscible Carbon Dioxide Flood. Paper No. – 159, presented in 4th UNITAR/UNDP International Conference on Heavy Crude and Tar Sands, August 7 – 12, Edmonton, Alberta, Canada.

Pujol, L. and Boberg, T.C. 1972. Scaling Accuracy of Laboratory Steam Flooding Models. SPE – 4191, presented in California Regional meeting of SPE of AIME, Bakersfield, California, November 8 – 10.

Pozzi, A. L. and Blackwell, R.J. 1963. Design of Laboratory Models for Study of Miscible Displacement. *Soc. Pet. Engg. J*. 4: 28 – 40.

Rojas, G.A. 1985. Scaled Model Studies of Immiscible Carbon Dioxide Displacement of Heavy Oil. PhD dissertation, Department of Mineral Engineering, U of Alberta, Edmonton, Alberta, Canada.

Sundaram, N.S. and Islam, M.R. 1994. Scaled Model Studies Petroleum Contaminant Removal from Soils Using Surfactant Solutions. *J. of Hazardous Materials*. 38: 89 – 103.